DESY 95-172
hep-ph/9509321
September 1995

ISSN 0418-9833

arXiv:hep-ph/9509321v1 18 Sep 1995

Inclusive Two–Jet Cross Sections in $\gamma\gamma$–Processes at e^+e^- Colliders

T. Kleinwort, G. Kramer
II. Institut für Theoretische Physik*
Universität Hamburg
D - 22761 Hamburg, Germany

Abstract

We have calculated inclusive one– and two–jet production in photon–photon collisions in next–to–leading order superimposing direct, single resolved and double resolved cross sections. The results are compared with recent experimental data from the TOPAZ and AMY collaborations at TRISTAN. Good agreement is found between experiment and the theoretical results.

*Supported by Bundesministerium für Forschung und Technologie, Bonn, Germany under Contract 05 6HH93P(5) and EEC Program "Human Capital and Mobility" through Network "Physics at High Energy Colliders" under Contract CHRX–CT93–0357 (DG12 COMA)

1 Introduction

Phenomena involving high transverse momenta (p_T) in γ–γ collisions with the incoming photons being real or quasi–real have been studied for many years now, both experimentally and theoretically. Emphasis has been on γ–γ collisions at relatively high center of mass energies in order to obtain information beyond the low p_T region which is determined by soft physics. This has been achieved recently at the TRISTAN [1, 2] and LEP [3] storage rings. Two TRISTAN collaborations, TOPAZ [1] and AMY [2] have presented data for inclusive one–jet and two–jet cross sections with p_T's up to 8 GeV. This is the domain of perturbative QCD calculations which are expected to be valid when there is a large energy scale in the interaction. Then the lowest order diagram is that of the quark parton model (QPM) (see Fig. 1a) also referred to as the direct contribution in leading order (LO) QCD. Here the two photons couple directly to the charge of the bare quark with no further interactions involved, so that the final state consists of just two jets. In next–to–leading order (NLO), i.e. $O(\alpha^2\alpha_s)$, there exists a contribution as, for example, the one in Fig. 1b where a gluon is emitted from the internal quark line. This contribution becomes singular when the momentum of the outgoing quark (antiquark) is collinear to the momentum of the upper (lower) photon. This divergent contribution is dealt with by introducing the scale dependent photon structure function at the upper or lower vertex. This leads to the so–called 'single resolved' (SR) contribution depicted in Fig. 1c in LO, being $O(\alpha\alpha_s)$, when the photon structure function is factored out. NLO corrections to the single resolved cross section, for example, produce contributions with a gluon emitted from the internal quark line in Fig. 1d which becomes singular in the collinear limit. These singular pieces are absorbed as before in the scale dependent photon structure function now at the lower (upper) vertex. This is the 'double resolved' contribution (DR) with photon structure functions at the upper and lower vertex, respectively, as shown in Fig. 1e. In addition to the two high p_T jets the single resolved (double resolved) contributions have one (two) low p_T "beam jets" or photon remnant jets. This was first discussed in the paper by Brodsky et al. [4] who showed that resolved photon cross sections are of the same order as from LO direct contributions, i.e. the QPM process. This work has recently be extended by Drees and Godbole [5].

In all these processes, direct (D), single resolved (SR) and double resolved (DR) there is a hard subprocess in which two partons scatter at high p_T which can be calculated in perturbative QCD. The subprocess cross sections are convoluted with luminosity functions that give the distributions of the virtual photons in an electron and one or two photon structure functions that give the distribution of quarks and gluons inside a photon. The topological structure of these cross sections is equivalent to cross sections for jet production in γp collisions. There the direct (resolved) process corresponds to the SR (DR) component in $\gamma\gamma$ collisions. The proton structure function must be replaced by the photon structure function.

In LO calculations the three cross sections, D, SR and DR are superimposed, and rates for topologies with two high p_T jets plus one or two photon remnant jets can be predicted. It is well known that LO calculations give only qualitative results. In this order the predictions depend highly on the factorization scale, in particular for the DR contribution. Furthermore LO results do not depend on any jet definition which is present in NLO and in the experimental data. Therefore all three processes must be treated in NLO, i.e. with higher order corrections included both in the photon structure function and the hard subprocesses in a consistent way. Such calculations were done by Aurenche et al. for the inclusive single–jet cross section at $\sqrt{S} = 58$ GeV [6]. They compared their results with the TOPAZ data [1] and found good argeement up to the highest p_T by slightly adjusting the non–perturbative input of the photon

structure function still consistent with the data on F_2^γ. Besides the inclusive one–jet data from TOPAZ [1] and AMY [2] there exist also measurements of the inclusive two–jet cross sections by the TOPAZ [1] and the AMY [2] collaborations. These data have been compared so far only to LO calculations by the authors assuming different sets of photon structure functions. In this work we make an effort to predict these two–jet cross sections in NLO assuming the same kinematical constraints as in the two TRISTAN experiments. Unfortunately we are not in the position yet to calculate all three components, the D, SR and DR cross sections up to NLO. We have only the NLO formalism for the direct and the single resolved cross section at our disposal. Since they yield, depending on p_T, the major part of the two–jet cross section at 58 GeV we shall estimate the DR cross section with a lowest order calculation including some k factor. This k factor is estimated with the inclusive one–jet cross section by comparing with the NLO prediction.

In section 2 we explain the formalism used to calculate the inclusive two–jet cross section. Section 3 contains the comparison with the TOPAZ and AMY data and a discussion of the results.

2 Inclusive Jet Cross Sections

As explained in the introduction the inclusive jet cross section at large p_T consists of three parts according to how the incoming photons take part in the hard subprocesses. If both photons couple to the quarks in the hard scattering one defines the direct cross section σ^D (see Fig. 1a). For example, the inclusive two–jet cross section has the following form:

$$\frac{d^3\sigma^D}{dp_T d\eta_1 d\eta_2} = \left(\frac{d^3\sigma^D(\gamma\gamma \to \mathrm{jet}_1 + \mathrm{jet}_2)}{dp_T d\eta_1 d\eta_2}\right)_{\mathrm{LO}} + \frac{\alpha_s(\mu)}{2\pi} K^D(R, M) \qquad (1)$$

In (1) p_T denotes the transverse momentum of the measured or trigger jet with rapidity η_1, η_2 is the rapidity of another jet such that in the three–jet sample these two jets have the highest and second highest p_T. The first term on the right–hand side of (1) stands for the LO cross section and the second term is the NLO correction which depends on the factorization scale M, at which the initial state collinear singularity is absorbed in the photon structure function. The variable R is the usual parameter defining the size of the jets with transverse momentum p_T, rapidity η and azimuthal angle ϕ. When two partons fulfill the snowmass constraint [7] with the cone size parameter R they are recombined in one jet. The same jet definition is used in the TOPAZ and AMY analysis.

The NLO corrections $K^D(R, M)$ are calculated with the phase–space slicing method using for the seperation of the $\gamma\gamma \to 2$ jets and $\gamma\gamma \to 3$ jets cross sections an invariant mass cut–off y, defined as $2p_i p_j < ys$, where s is the partonic center of mass energy squared. In the direct process the cross section for $\gamma\gamma \to q\bar{q}g$ has soft, initial and final state collinear singularities. The $\gamma\gamma \to q\bar{q}g$ cross section is integrated over these singular regions up to the cut–off value y which isolates the respective singularities which are cancelled against the singular contributions of the virtual corrections to $\gamma\gamma \to q\bar{q}$ and the subtraction term at the scale M which are absorbed into the photon structure function. Outside the cut–off region controlled by the parameter y we have genuine $q\bar{q}g$ final states. In this contribution two of the partons are recombined if they obey the snowmass constraint. The LO contribution and the NLO correction inside the y cut–off contribute to the two–jet cross section together with the contributions inside the cone with radius R. That part of the $q\bar{q}g$ contribution not fulfilling the cone recombination condition

stands for the 3–jet cross section of which we have calculated the inclusive two–jet cross section as a function of p_T, η_1 and η_2 where p_T is the transverse momentum of the measured jet or trigger jet with rapidity η_1 and η_2 is the rapidity of another jet so that both p_{T1} and p_{T2} are the jets with highest p_T. For the two–jet cross section $p_{T1} = p_{T2}$. This inclusive cross section is independent of the invariant mass parameter y used to seperate those regions of phase space that contain the soft and collinear singularities. However the inclusive two–jet cross section depends on the cone size R.

If one of the two incoming photons interacts via the quark or the gluon component in its structure function we define

$$\begin{aligned}
&\frac{d^3\sigma^{SR}}{dp_T d\eta_1 d\eta_2} = \\
&\sum_{i=q,g} \int dx_1 F_{i/\gamma}(x_1, M) \left(\left(\frac{d^3\sigma^{SR}(i\gamma \to \text{jet}_1 + \text{jet}_2)}{dp_T d\eta_1 \eta_2} \right)_{LO} + \frac{\alpha_s(\mu)}{2\pi} K_{i\gamma}^{SR}(R, M, \mu) \right) \\
+ &\sum_{i=q,g} \int dx_2 F_{i/\gamma}(x_2, M) \left(\left(\frac{d^3\sigma^{SR}(\gamma i \to \text{jet}_1 + \text{jet}_2)}{dp_T d\eta_1 \eta_2} \right)_{LO} + \frac{\alpha_s(\mu)}{2\pi} K_{\gamma i}^{SR}(R, M, \mu) \right) \qquad (2)
\end{aligned}$$

This cross section has the same structure as the direct inclusive two–jet cross section for photoproduction $\gamma p \to \text{jet}_1 + \text{jet}_2 + X$, where the photon structure function in (2) is replaced by the proton structure function. This cross section has been calculated recently with the phase space slicing method with invariant mass cut slicing [8]. The developed formulas for the two–jet photoproduction cross section can be transformed easily to the corresponding γ–γ process. The first term in each bracket of (2) is the LO cross section and $K_{i\gamma}^{SR}$, $K_{\gamma i}^{SR}$ stand for the NLO corrections which depend on R and the two scales μ (renormalization) and M (factorization). The cross section in (2) has two separate terms, depending whether the first or the second photon interacts through its structure function $F_{i/\gamma}$.

When both photons are resolved we have

$$\begin{aligned}
\frac{d^3\sigma^{DR}}{dp_T d\eta_1 d\eta_2} &= \sum_{i,j=q,g} \int dx_1 \int dx_2 F_{i/\gamma}(x_1, M) F_{j/\gamma}(x_2, M) \\
&\left(\left(\frac{d^3\sigma^{DR}(ij \to \text{jet}_1 + \text{jet}_2)}{dp_T d\eta_1 d\eta_2} \right)_{LO} + \frac{\alpha_s(\mu)}{2\pi} K_{ij}^{DR}(R, M, \mu) \right) \qquad (3)
\end{aligned}$$

This cross section has the same structure as the NLO resolved inclusive two–jet cross section for photoproduction $\gamma p \to \text{jet}_1 + \text{jet}_2 + X$, where the photon structure function at one vertex is replaced by the proton structure function. For this cross section the higher order corrections $K_{ij}^{DR}(R, M, \mu)$ have not been calculated yet. However they are available for the inclusive single–jet cross section [9] and are transformed to the γ–γ case. Concerning the inclusive two–jet cross section in the double resolved case our strategy is as follows. First we have calculated the inclusive one–jet cross section in NLO, i.e. with the terms K_{ij}^{DR}, and have compared it with the LO cross section, so that we know the k factor for the one–jet cross section. The same k factor is applied to the two–jet cross section which is calculated in LO only. Since for $p_T \geq 4$ GeV the DR contribution is less than 20% this estimate of the two–jet double resolved cross section is sufficient.

It is obvious that the NLO corrections K^D, $K_{i\gamma}^{SR}$ and K_{ij}^{DR} in (1), (2) and (3) depend on the same kinematic variables p_T, η_1 and η_2 as the LO cross sections. We specified only the dependence on the cone size R, on the factorization scale M and on the renormalization scale μ.

Before we compare our results with the TOPAZ and AMY data we have made some tests of the NLO corrections to the one– and two–jet cross sections. First we checked that these cross sections are independent of the cut–off y if y is chosen small enough. This was the case for $y < 10^{-3}$ in all considered cases. For y above 10^{-3} we observed some small y dependence which is caused by our approximation that we neglected contributions $O(y)$ in the analytical contribution to the two–jet cross section.

Second we tested that, first, the sum of NLO direct and the LO single resolved cross section and, second, the sum of the NLO single resolved cross section and the LO double resolved cross section are independent of the factorization scale M. This test was performed for the one– and two–jet cross section seperately under kinematic conditions as for the TOPAZ data. Similar checks were done earlier for the photoproduction one–jet cross section [10].

3 Comparison with TOPAZ and AMY Data

In e^+e^- collisions at TRISTAN the jets are produced via the exchange of two quasi–real photons. The spectrum of these small Q^2 photons is described by the Weizsäcker–Williams approximation

$$F_{\gamma/e}(z,E) \;=\; \frac{\alpha}{\pi}\frac{(1+(1-z)^2)}{z}\ln\left(\frac{E\Theta_{\max}(1-z)}{m_e z}\right) \tag{4}$$

where $\Theta_{\max}$ is the maximally allowed angle of the electron (positron) which experimentally is realized by the anti–tagging counters. E is the beam energy of the electron (positron) and $z = E_\gamma/E$ is the fraction of electron (positron) energy transferred to the respective photon.

In this approximation the inclusive two–jet cross section $e^+ + e^- \to e^+ + e^- + \mathrm{jet}_1 + \mathrm{jet}_2 + X$ is obtained from

$$\frac{d^3\sigma(e^+ + e^- \to e^+ + e^- + \mathrm{jet}_1 + \mathrm{jet}_2 + X)}{dp_T d\eta_1 d\eta_2} = \int dz_1 \int dz_2 F_{\gamma/e}(z_1,E) F_{\gamma/e}(z_2,E)\,\frac{d^3\sigma(\gamma+\gamma \to \mathrm{jet}_1 + \mathrm{jet}_2 + X)}{dp_T d\eta_1 d\eta_2} \tag{5}$$

where the cross section on the right–hand side stands for the interaction between two real photons.

Depending on the experimental conditions we encounter specific values for $\Theta_{\max}$ and eventually for the integration range of z_1 and z_2, respectively, in (5).

Before presenting the results we must specify the parton distributions in the photon, $F_{i/\gamma}$, which appear in (2) and (3). We have chosen the NLO set of Glück, Reya and Vogt (GRV) in the $\overline{\mathrm{MS}}$ scheme [11]. In [11] the photon structure function is given in the so–called DIS_γ scheme. The transformation to the $\overline{\mathrm{MS}}$ scheme is known and given in [11]. This means that the direct, single resolved and double resolved cross section must also be calculated with the $\overline{\mathrm{MS}}$ subtraction. We have tested that the DIS_γ scheme for the photon structure function of GRV leads to the same results. We choose all scales $\mu = M = p_T$ and calculate α_s from the two–loop formula with $N_f = 4$ massless flavours with $\Lambda_{\overline{\mathrm{MS}}} = 0.2$ GeV equal to the Λ value of the NLO GRV photon structure function. The charm quark is treated also as a light flavour with the boundary condition that the charm content of the photon structure function vanishes for $M^2 \le {m_c}^2$ ($m_c = 1.5$ GeV).

The TOPAZ data are obtained for $\Theta_{\max} = 3.2^\circ$ and z_1, $z_2 \le 0.75$ [1]. The rapidities of the two jets are restricted to $|\eta_1|$, $|\eta_2| \le 0.7$ and $R = 1$. The same input is used for the calculations

of the NLO cross sections. Our result for the inclusive single jet cross sections $d\sigma(\text{one–jet})/dp_T$ is shown as a function of p_T in Fig. 2a. We show four curves, the direct, single resolved, double resolved and the sum of all three components. All three cross sections are calculated up to NLO and the curve for the sum should be compared with the TOPAZ points. The agreement is good at small p_T. At larger p_T, where the theory is more trustworthy, the theoretical curve falls off stronger with increasing p_T than the data. The error bars on the data include both statistical and systematic uncertainties. The effects of the NLO corrections are as follows. If we compare with the LO result, where only the NLO corrections in the hard scattering are removed, i.e. the LO cross section is calculated with the same NLO GRV photon structure function as in the NLO computation we encounter the following k factors: $k \simeq 0.9$ (direct), $k \simeq 1.1$ (single resolved), $k \simeq 1.9$ (double resolved) and $k \simeq 1.0$ (sum)[1]. We emphasize that the k factor depends on the way the LO cross section is evaluated. If we use in LO the one–loop α_s with the same Λ value the k factors are: $k \simeq 0.9$ (D), $k \simeq 0.9$ (SR), $k \simeq 1.2$ (DR) and $k \simeq 0.9$ (sum). In Fig. 2b we have plotted the two–jet cross section $d\sigma(\text{two–jet})/dp_T$ as a function of p_T. We show again the direct, single resolved, double resolved cross section and the sum of all three contributions. Over the whole range of p_T the agreement with the TOPAZ data is excellent. We notice that the double resolved cross section falls off with p_T somewhat stronger in relation to the direct and single resolved components as in the one–jet cross section. The double resolved cross section is calculated in LO with the same k–factor as obtained in the inclusive one–jet cross section. For the direct and single resolved cross section the k factors for the one– and two–jet cross section are approximately equal, so that we can expect this also for the double resolved cross section.

The same plots but now with the kinematical contraints of the AMY experimental data, $\Theta_{\max} = 13^\circ$, $z_1,\ z_2 \leq 1$ and $|\eta| \leq 1$ for the one–jet cross section and $|\eta_1|,\ |\eta_2| \leq 1$ for the two–jet cross section are shown in Fig. 3a,b. All other input is as for the TOPAZ curves. The k factors are the same as for the TOPAZ cross sections. The agreement between theory and experiment for the one–jet data is somewhat better than in the TOPAZ case. The low and high p_T data points agree quite well. Only in the intermediate range $3 < p_T < 5$ GeV the measured cross section is smaller than the predicted cross section. The two–jet cross section agrees very well with the data for all p_T. We observe that for both experiments the two–jet data agree somewhat better with our prediction than the one–jet data. This shows that the NLO cross sections correctly account for the experimental data. Also the GRV photon structure function which gives a good fit of existing inelastic $e\gamma$ scattering data produces the correct description of the single resolved and double resolved cross sections. Before stronger conclusions can be drawn from the comparison one should investigate several effects that could influence our predictions. Most of them would change the cross section noticeable only at small $p_T \leq 3$ GeV. Such effects are, for example, corrections to the Weizsäcker–Williams approximation. Part of these corrections have been studied in [12], including intrinsic p_T effects caused by the non–zero momentum of the virtual photons. Other corrections come from the non–vanishing charm mass or non–perturbative intrinsic p_T effects in the photon structure functions. All these corrections, as far as they have been estimated [6, 12], are below the experimental errors and most of them are relevant only at small p_T.

[1]These are the k factors for the special cone radius $R = 1$. For smaller or larger cone radii the k factors would be completely different [9].

4 Conclusions

Differential inclusive single– and dijet cross sections $d\sigma/dp_T$ have been calculated in NLO for the direct, single resolved and double resolved component as a function of p_T. For the double resolved two–jet cross section the NLO corrections are estimated with a k factor taken from the inclusive one–jet cross section. The sum of these cross sections are compared to the TOPAZ and AMY experimental data. We obtained good agreement between measured data and the theoretical predictions. For both experiments the two–jet data seem to agree better with the theory, than the one–jet data which may be due to the larger experimental errors of the two–jet data. The single and double resolved cross sections are obtained with the GRV photon structure function which gives also good overall agreement with all measurements on F_2^γ. At large p_T the direct and the single resolved components are the most important ones, so that only at smaller p_T the photon structure function can be constrained by the double resolved component.

References

[1] H. Hayashii et al., TOPAZ Collaboration, Phys. Lett. B314 (1993) 149.

[2] B. J. Kim et al., AMY Collaboration, Phys. Lett. B325 (1994) 248.

[3] D. Buskulic et al., ALEPH Collaboration, Phys. Lett. B313 (1993) 509,
R. Akers et al., OPAL Collaboration, Z. Phys. C61 (1994) 199,
P. Abreu et al., DELPHI Collaboration, Z. Phys. C62 (1994) 357.

[4] S. J. Brodsky, T. DeGrand, J. Gunion, J. Weis, Phys. Rev. D19 (1979) 1418.

[5] M. Drees, R. M. Godbole, Nucl. Phys. B339 (1990) 355.

[6] P. Aurenche, J. Ph. Guillet, M. Fontannaz, Y. Shimizu, J. Fujimoto,
Progr. Theor. Phys. 92 (1994) 175.

[7] J. E. Huth et al., Proceedings of the 1990 DPF Summer Study on High Energy Physics, Snowmass, Colorado, edited by E. L. Berger, World Scientific, Singapore, 1992, p. 134.

[8] M. Klasen, G. Kramer, DESY 95–195, August 1995.

[9] G. Kramer, S. G. Salesch Z. Phys. C61 (1994) 277,
S. G. Salesch, DESY 93–196, December 1993.

[10] D. Bödecker, G. Kramer, S. G. Salesch, Z. Phys. C63 (1994) 471.

[11] M. Glück, E. Reya, A. Vogt, Phys. Rev. D45 (1992) 3986,
M. Glück, E. Reya, A. Vogt, Phys. Rev. D46 (1992) 1973.

[12] P. Aurenche, J.–Ph. Guillet, M. Fontannaz, Y. Shimizu, J. Fujimoto, K. Kato, Proc. of the Workshop on Two–Photon Physics at LEP and HERA, Lund, Eds. G. Jarlskog and L. Jönsson, Lund Univ., 1994, p. 269.

5 Figure Caption

Fig. 1: Generic diagrams for jet production in γ–γ collisions: (a) direct production in LO, (b) direct production in NLO, (c) single resolved production in LO, (d) single resolved production in NLO and (e) double resolved production in LO.

Fig. 2: $d\sigma/dp_T$ with $R = 1$ as a function of p_T for direct (dashed), single resolved (dashed–dotted) and double resolved (dotted) production in NLO. Full curve is the sum of all three components compared to TOPAZ data [1]:

(a) Inclusive one–jet cross section with $\eta < 0.7$, $\Theta_{\max} = 3.2°$.

(b) Inclusive one–jet cross section with η_1, $\eta_2 < 0.7$, $\Theta_{\max} = 3.2°$.

The error bars on the data include both statistical and systematic uncertainties.

Fig. 3: $d\sigma/dp_T$ with $R = 1$ as a function of p_T for direct (dashed), single resolved (dashed–dotted) and double resolved (dotted) production in NLO. Full curve is the sum of all three components compared to AMY data [2]:

(a) Inclusive one–jet cross section with $\eta < 1.0$, $\Theta_{\max} = 13°$.

(b) Inclusive one–jet cross section with η_1, $\eta_2 < 1.0$, $\Theta_{\max} = 13°$.

The error bars on the data include both statistical and systematic uncertainties.

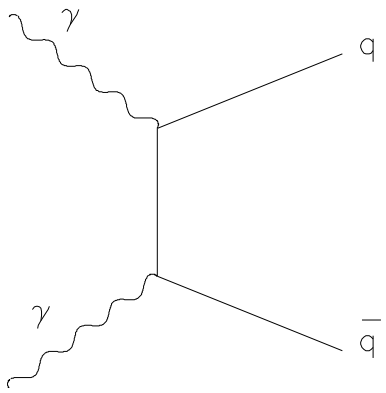

(a)

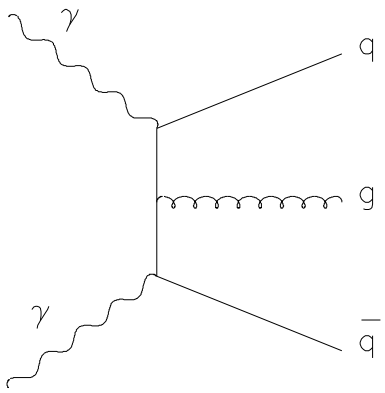

(b)

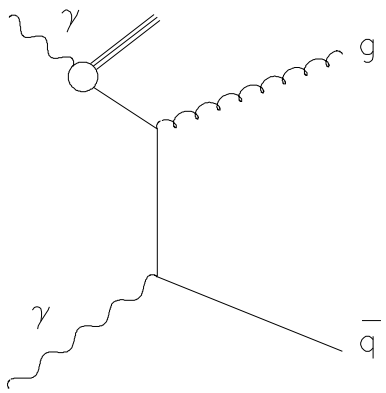

(c)

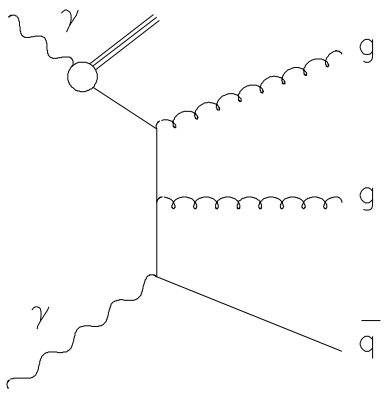

(d)

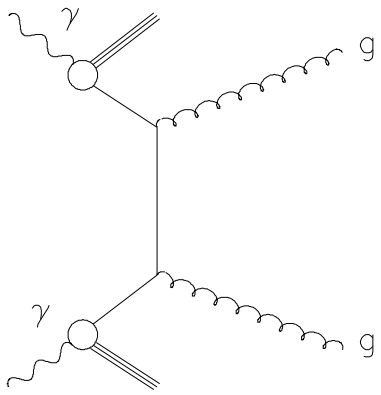

(e)

Fig. 1 a-e

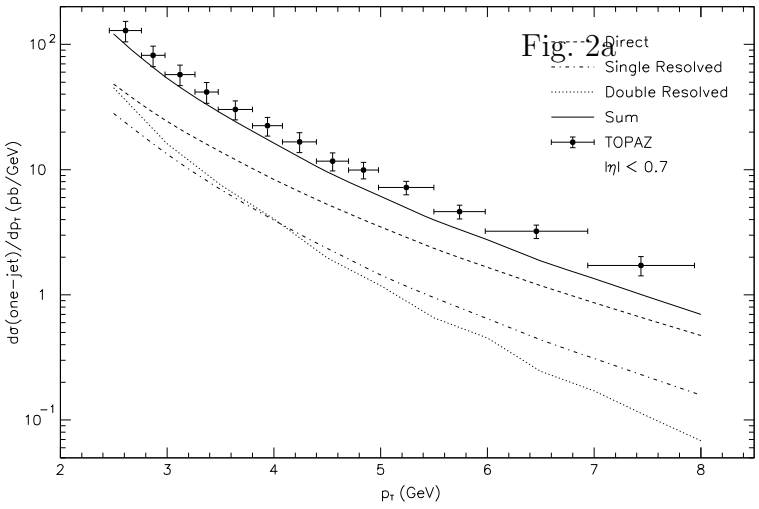
Direct
Single Resolved
Double Resolved
Sum
TOPAZ
|η| < 0.7
dσ(one−jet)/dp_T (pb/GeV)
p_T (GeV)

Fig. 2a

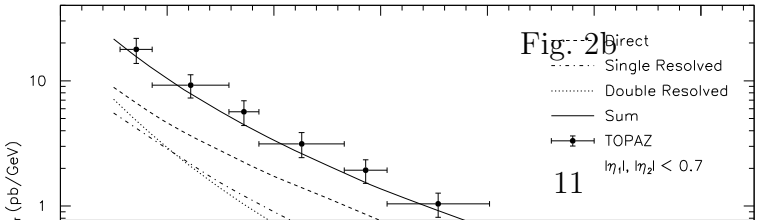
Direct
Single Resolved
Double Resolved
Sum
TOPAZ
|η_1|, |η_2| < 0.7

Fig. 2b

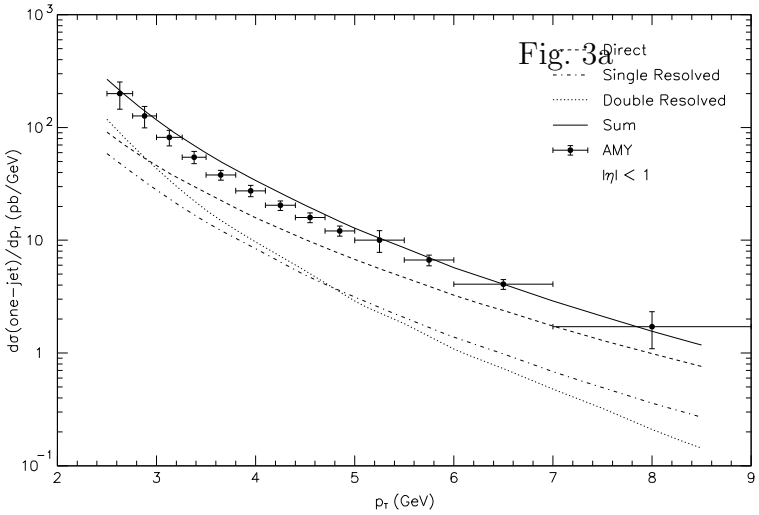
Direct
Single Resolved
Double Resolved
Sum
AMY
|η| < 1
dσ(one−jet)/dp_T (pb/GeV)
p_T (GeV)

Fig. 3a

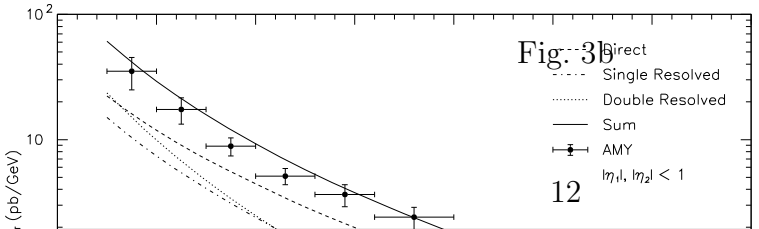
Direct
Single Resolved
Double Resolved
Sum
AMY
|η₁|, |η₂| < 1

Fig. 3b